Available online at www.sciencedirect.com
ScienceDirect
Nuclear Physics B (Proc. Suppl.) 187 (2009) 29–35
NUCLEAR PHYSICS B PROCEEDINGS SUPPLEMENTS
www.elsevierphysics.com

Two measurements of ππ scattering lengths a_0 and a_2 from studies of $K^{\pm}$ decays with the CERN-NA48/2 experiment.

Bernard Peyaud
CEA-Saclay, IRFU, Gif sur Yvette 91191 Cedex France.
(On behalf of the NA48 collaboration)

Abstract. The NA48 experiment at the CERN SPS has used K_L^0 and K_S^0 kaons for the precise measurement of the direct CP violation parameter Re(ε'/ε). In 2002 it was re-designed as NA48/2 to search for CP violation in $K^{\pm} \to 3\pi$ decays. This configuration has also allowed studying several rare decay processes of charged kaons to test chiral perturbation theory. With data samples of ~10^6 $K^{\pm}\to\pi^{\pm}\pi^{-}e^{\pm}\nu$ decays, precise values of a_0 and a_2, the isospin I=0 and I=2 *s*-wave ππ scattering lengths, are extracted with an unprecedented experimental precision. The same scattering lengths are also measured using ~60x10^6 $K^{\pm}\to\pi^{\pm}\pi^0\pi^0$ decays where a cusp structure in the Dalitz plot has been observed for the first time.

1. The NA48/2 beam-line and detector

The experimental setup used by NA48/2 is made of a modified beam line and improved NA48 detector [1]. The new beam line provides simultaneous and collinear positive and negative kaons beams at high intensity. The production of charged particles beams is made by 400GeV/c protons from the CERN/SPS interacting on a Beryllium target. These secondary charged particles, mostly pions, are selected in a dedicated achromatic system in which $K^+(K^-)$ of about 2(1)x10^6particles/pulse have the same momentum of 60GeV/c±3GeV/c(rms). The experimental setup provides superimposed beams coinciding within 1mm along the 114m evacuated decay volume in front of the detector (Figure 1).

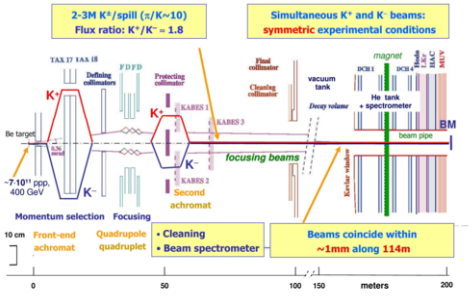

Fig 1: Schematics of the NA48/2 experiment using high intensity beams of charged kaons.

The experiment has operated these intense beams during two runs of 50 and 60 days to measure primarily the Dalitz plot properties of charged kaons using the $K^{\pm}\to\pi^{\pm}\pi^{+}\pi^{-}$ and $K^{\pm}\to\pi^{\pm}\pi^0\pi^0$ decays modes in a search for direct CP violation [1]. For the studies presented here on $K^{\pm}\to\pi^{\pm}\pi^{-}e^{\pm}\nu$ and $K^{\pm}\to\pi^{\pm}\pi^0\pi^0$ decays the important detector elements are the magnetic spectrometer, the liquid krypton (LKr) electromagnetic calorimeter and the muon veto counter.

The magnetic spectrometer consists of four drift chambers and a dipole magnet giving a transverse momentum kick of P_t=120 MeV/c. It provides an accurate measurement of 150μm of hits from charged tracks positions resulting in a resolution on their momentum P which is parameterized as $\sigma(P)/P = [1.0 \oplus 0.044P(GeV/c)]\%$.

The 21 tons of LKr at 112K in the cryostat of the electromagnetic calorimeter is the ionizing material of $27X_0$ that allows measuring the energy E of photons from $\pi^0\to\gamma\gamma$ decays with $\sigma(E)/E = 3.2\%/\sqrt{E} \oplus 9\%/E \oplus 0.42\%$ (E in GeV).

The muon veto counters installed at the end of the detector are composed of flat strips of NE110 plastic scintillator arranged in 3 planes, each one being preceded by 80cm thick iron wall to absorb hadrons. The data sets that are discussed in this paper are those recorded during the entire run periods of 2003 and 2004.

The interest of the rare decays $K^{\pm}\to\pi^{\pm}\pi^{-}e^{\pm}\nu$, called K_{e4}, with branching ratio BR= (4.09±0.10)x10^{-5} is two fold: it provides information on the structure of the weak hadronic currents and on ππ scattering at very low energies just above the production

doi:10.1016/j.nuclphysbps.2009.01.005

threshold. It is a clean environment for studying strong interaction since the 2 pions are the only hadrons in the final state. The very large statistics of the $K^{\pm}\to\pi^{\pm}\pi^0\pi^0$ decays which have BR=(1.757±0.024)% allows to look at fine details in the corresponding Dalitz plots. The study of the cusp structure discovered in the invariant mass of the $\pi^0\pi^0$ system around $(m_{\pi^+}+m_{\pi^-})$ offers another handle to understand in detail the mechanism of $\pi^+\pi^-$ re-scattering. Both K_{e4} and $K^{\pm}\to\pi^{\pm}\pi^0\pi^0$ decays are used for the measurement of the scattering lengths a_0 and a_2 that have been accurately predicted in the framework of chiral perturbation theory.

2. The rare and rich K_{e4} decays.

2.1. Data selection.

The selection of events from K_{e4} semi-leptonic decays is made from events reconstructed with 3 charged tracks in time within 2ns with the hodoscope signals. Each one of the two pions, π^+ and π^-, is identified with E/P<0.8 and the positron(electron) in $K^+(K^-)$ with 0.9<E/P<1.1. The closest distance of approach of the tracks is used to determine the vertex of the decay which in turn allows measuring the transverse momentum P_t of the 3 tracks together with respect to the kaon line of flight. Assuming that the tracks are all pions their invariant mass $M_{3\pi}$ is used with P_t to reject $K\to3\pi$ background that fakes K_{e4} when one of the pion is misidentified as an electron. The other background sources are from $K^{\pm}\to\pi^{\pm}\pi^+\pi^-$ and subsequent $\pi\to e\nu$ decay and from $K^{\pm}\to\pi^{\pm}\pi^0(\pi^0)$ with $\pi^0\to e^+e^-\gamma$ and e/π misidentification plus undetected γ. With the cuts chosen for the K_{e4} selection the background level is typically at 0.5% and the signals from K_{e4} decays are very clean (Figure 2).

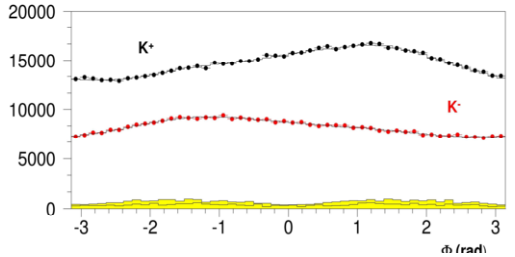

Fig 2: Distributions of the ϕ angle between the ππ pair and the eν pair for K_{e4} decays of K^+ and K^-. The 0.5% background shown in yellow is scaled by 10.

The total number of K_{e4} decays selected during the runs of 2003 and 2004 and used in the analysis amounts to 739500 K^+ events and 411000 K^- events. Over the last 30 years only a handful of experiments have been studying this decay channel and the very high statistics accumulated by NA48/2 represents 40 times the early dedicated measurement [3] on K_{e4} and about two times the data accumulated by the last experiment [4].

2.2. Kinematics and simulation.

The K_{e4} decay is described by the following conventional set of five kinematic variables, introduced by Cabibbo and Maksymowicz [5], the invariant masses $M_{\pi\pi}$ and M_{ev} of the dipion $(\pi^+\pi^-)$ and of the dilepton $(e^{\pm}\nu)$, the angles θ_π and θ_e to characterize the "decay" of the dipion and of the dilepton in their respective rest frames and the oriented angle ϕ between the normals to the planes defined by the dipion and the dilepton as illustrated in Figure 3.

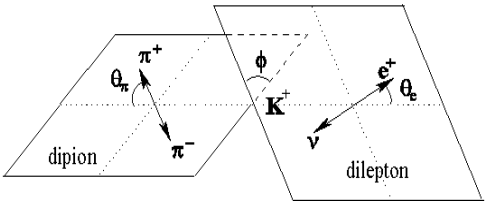

Fig3: The five variables used to describe the kinematics of K_{e4} decays.

The detailed Monte Carlo simulation using GEANT3 taking into account the incident $K^+(K^-)$ trajectories and their time dependence has been used to show that the dominant part of the background is from $\pi\to e\nu_e$ decay of $K^{\pm}\to\pi^{\pm}\pi^+\pi^-$ events. These events also produces *wrong sign* K_{e4} *like* decays $K^+(K^-)\to\pi^+\pi^-e^-(e^+)\ \bar{\nu}_e(\nu_e)$ recorded in the detector that are used as a powerful tool to subtract the background in the 5 dimensional kinematic space. From combinatorial counting of electric charges it is obvious that the amount of background of this type remaining with the K_{e4} signal is twice as much as the observed *wrong sign* events.

The transition amplitude for K_{e4} decay is governed by the vector and axial-vector coupling of the leptons to hadronic currents [6] and it is practical to use three form factors F, G and H to describe the dynamics of the process. Our analysis uses the standard Pais-Treiman parameterization [7] which is done with the assumption of time-reversal invariance and using a partial wave expansion of the form factors with respect to the angular momentum of the dipion system. With very good accuracy it is sufficient to take into account *l=0* and *l=1* waves

only and F, G, H read $F = F_s e^{i\delta_s} + F_p e^{i\delta_p} \cos\theta_\pi$, $G = G_p e^{i\delta_p}$ and $H = H_p e^{i\delta_p}$ respectively. The quantities, F_s, F_p, G_p and H_p, depend potentially on $M_{\pi\pi}$ and M_{ev} while the phase shift observable $\delta_{\pi\pi} = \delta_p - \delta_s$, in which direct strong-interaction information is inscribed, depends on $M_{\pi\pi}$ only. The probability of the K_{e4} decay is written as:

$$d^5w \propto \rho I dM_{\pi\pi}^2 dM_{ev}^2 d(\cos\theta_\pi) d(\cos\theta_e) d\phi$$

where the phase space factor ρ depends only on $M_{\pi\pi}$ and M_{ev} and where the intensity distribution I has a calculable structure that factorizes in the angular variables θ_e and ϕ as:

$$I = I_1 + I_2\cos 2\theta_e + I_3 \sin^2\theta_e \cos 2\phi + I_4 \sin 2\theta_e \cos\phi + I_5 \sin\theta_e \cos\phi + I_6 \cos\theta_e + I_7 \sin\theta_e \sin\phi + I_8 \sin 2\theta_e \sin\phi + I_9 \sin^2\theta_e \sin 2\phi$$

In this distribution each I_i coefficient is a product of 2 interfering form factors and is a function of the 3 quantities $M_{\pi\pi}$, M_{ev}, θ_π. It is important to remark that the phase shift $\delta_{\pi\pi}$ enters directly in I_7 with the form $I_7 \propto F_s G_p \sin\delta_{\pi\pi}$ representing the interference between F_s and G_p. This is the dominant $\sin\phi$ component of the spectral function I introducing the asymmetries in the ϕ distribution of K^+ and K^- seen in Figure 2. These asymmetries, although being the observed ones, are not significantly changed by the detector acceptances which have a mild even dependence versus ϕ.

2.3. Fitting the data.

The fits are made separately for K^+ and K^- that are binned in 10 independent subdivisions of $M_{\pi\pi}$ chosen with equal statistics. The four dimensional sub-space in M_{ev}, $\cos\theta_\pi$, $\cos\theta_e$ and ϕ for each $M_{\pi\pi}$ bin is in turn subdivided in 5x5x5x12 equally populated cells with 49 events/cell for K^+ and 27 events/cell for K^-. The fitting procedure makes use of a dedicated estimator taking into account Poisson fluctuations of the number of events in the cells. The expected events are simulated by Monte Carlo with about 25 times the data statistics. It uses a realistic K_{e4} matrix element with treatment of radiative corrections by PHOTOS and takes into account Coulomb effects. The procedure takes advantage of the factorization of the physics imbedded in the I coefficients and calculates the best set of parameters F_S, F_p, G_P, H_P and $\delta_{\pi\pi}$ minimizing the difference between observed and expected events in the 1500 boxes. The K^+ and K^- are in the ratio of 1.8 to 1 and the two sets are averaged to obtain $\delta_{\pi\pi}$ and the form factors (normalized to F_S) in each $M_{\pi\pi}$ bin.

For completeness the form factors in the fit are allowed to depend on $q_\pi^2 = (M_{\pi\pi}/2m_\pi)^2 - 1$ and $q_e^2 = (M_{ev}/2m_\pi)^2$ with, $F_p = f_p + f_p' q_\pi^2$, $F_s = f_s + f_s' q_\pi^2 + f_s'' q_\pi^4 + f_e' q_e^2$, $G_p = g_p + g_p' q_\pi^2$ and $H_p = h_p + h_p' q_\pi^2$ giving the results in Table 1:

Form factor	value stat. syst.
f'_s/f_s	0.158 ± 0.007 ± 0.006
f''_s/f_s	-0.078 ± 0.007 ± 0.007
f'_e/f_s	0.067 ± 0.006 ± 0.009
f_p/f_s	-0.049 ± 0.003 ± 0.004
g_p/f_s	0.869 ± 0.010 ± 0.012
g'_p/f_s	0.087 ± 0.017 ± 0.015
h_p/f_s	-0.402 ±0.014 ± 0.008

Table1: K_{e4} form factors obtained from the combination of K^+ and K^-. The systematic errors are from the 2003 run.

The form factors F_p and H_p are constant while G_p increases moderately as function of $M_{\pi\pi}$. The measurement of f_p/f_s = -0.049±0.005 is the first observation of non zero value of the F_p form factor.

Various sources of systematic errors have been studied with the data set of 2003. They include variations of the fit method, trigger inefficiencies, acceptances uncertainties and change of background shape, electron identification, radiative corrections uncertainties, background level and q_e dependence through f_e'. For most of the fitted parameters the last two sources give the larger systematic effects.

Furthermore, this procedure gives for each $M_{\pi\pi}$ bin a model independent measurement of $\delta_{\pi\pi}$. These results are shown by the open circles in Figure 4.

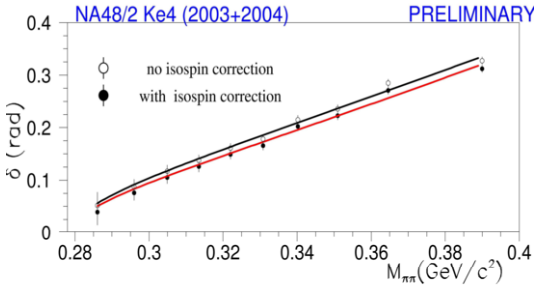

Fig 4: The phase shift $\delta_{\pi\pi}$ as function of $M_{\pi\pi}$ measured with K_{e4}. The isospin correction changes the open circles into the black ones.

Nevertheless in order to be used for the extraction of a_0 and a_2 the measured ππ phase shifts need to be corrected for isospin breaking effects as calculated in [8]. For the most part this correction boils down to a shift of ~12mrad on $\delta_{\pi\pi}$ giving the black circles in figure 4.

The relation between the phase shift $\delta_{\pi\pi}$ and the scattering lengths a_0 and a_2 is established by a set of dispersion relations contained in the Roy equations [9] in which the analytical properties and crossing symmetry of amplitudes are used. With the constraint from experimental measurements of ππ amplitudes made at energies above 800MeV the allowed range of predicted (a_0, a_2) values is bounded inside the Universal Band (UB) shown in figure 5. In the recent treatments [10], [11], [12] of this problem the Roy equations are solved numerically using an advanced parameterization of the phase shift, that allows to translate low energy data on scattering amplitudes into values for the scattering lengths.

Taking the central line of UB as a constraint the one parameter fit of a_0 to the isospin corrected $\delta_{\pi\pi}$ data gives:

$$a_0 = 0.234 \pm 0.005(stat) \pm 0.002(syst)$$

and $a_2 = -0.035 \pm 0.001$ UB constraint

The chiral perturbation theory (χPT) representation of ππ scattering lengths made at the 2 loop level has also been completed. It constrains (a_0, a_2) in the χPT band of figure 5 and the fit result is:

$$a_0 = 0.220 \pm 0.005(stat) \pm 0.002(syst)$$

and $a_2 = -0.0444 \pm 0.0011$ constraint

Finally, by performing a fit with both parameters a_0 and a_2 as parameters the result is:

$$a_0 = 0.218 \pm 0.013(stat) \pm 0.007(syst)$$

and $a_2 = -0.0457 \pm 0.0084 \pm 0.0041(syst)$

The correlation coefficient between a_0 and a_2 is 96% as indicated by the 68% CL ellipses in figure 5.

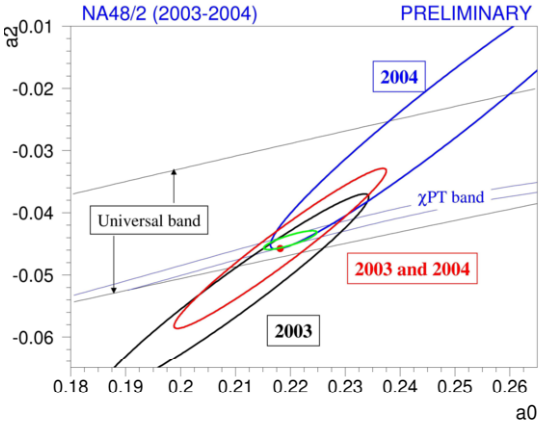

Fig 5: The scattering lengths (a_0, a_2) extracted from $\delta_{\pi\pi}$ measured with K_{e4}. The black (blue) ellipse corresponds to the 2003 (2004) runs and the red one to their combination. The UB (χPT) band is shown by the quasi parallel black (blue) lines.

The systematic errors are still conservatively kept at the level obtained with the 2003 data set. They will be revisited with the entire statistics and their sizes will remain significantly below the statistical ones.

The 2 parameter fit is feasible and meaningful thanks to the very large statistics and the experimental result is in excellent agreement with the χPT calculation that predicts $a_0 = 0.220 \pm 0.005$ and $a_2 = -0.0444 \pm 0.0008$ as shown by the green ellipse in figure 5.

3. The subtle cusp in $K \to \pi^{\pm}\pi^0\pi^0$ decays.

3.1. Selection of events.

The events are selected from triggers with at least one charged particle track and at least four γ energy clusters in LKr. To ensure that they are from the same event the time separation between the track and the photons is required to be within the experimental resolution of 1.5ns. Assuming that each possible pair (ij) of photons is from $\pi^0 \to \gamma\gamma$

decay the distance between the decay vertex and the LKr is calculated with:

$$D_{ij} = \sqrt{E_i E_j [(x_i - x_j)^2 + (y_i - y_j)^2]} \Big/ m_{\pi^0}$$

Where E_i , E_j are the energies of photons *i*, *j* respectively, and x_i, x_j, y_i, y_j their impact point coordinates on LKr. The photon pairs *(ij)* and *(kl)* with the smallest difference $D_{ij} - D_{kl}$ selects the combination consistent with the hypothesis of two π^0 from $K^{\pm}\to\pi^{\pm}\pi^0\pi^0$ decay and gives the best $\pi^0\pi^0$ mass resolution near threshold.

3.2. Cusp unveiled and interpreted.

The analysis of $K^{\pm}\to\pi^{\pm}\pi^0\pi^0$ decays was first made with 16×10^6 events of the 2003 run. This data set was sufficient to establish [13] that a sudden change of slope exists in M_{00}, the invariant mass of the $\pi^0\pi^0$ pair, in the vicinity of the threshold at $M_{00} = m_{\pi^+} + m_{\pi^-}$. This cusp structure is interpreted [14] in terms of decays that are originally *born* as $K^{\pm}\to\pi^{\pm}\pi^+\pi^-$ and in which one of the $\pi^+\pi^-$ pair undergoes electromagnetic effects and materializes as $\pi^0\pi^0$ in the final state. The 2004 run with 44×10^6 events shown in figure 6 is now added to the original sample and the analysis is done with improved selection criteria which allow reducing the sensitivity of the result to the Monte-Carlo simulation.

The Lorentz-invariant variables in use for the parameterization of M, the matrix element of the $K^{\pm}\to\pi^{\pm}\pi^0\pi^0$ decay, are $u = (s_3 - s_0)/m^2_{\pi^+}$ where $s_0 = (s_1 + s_2 + s_3)/3$ with $s_i = (P_K - P_i)^2$ and (i=1,2,3) for $(\pi^0, \pi^0, \pi^{\pm})$ and where P_K (P_i) is the K (π) four-momentum. The contribution from the $K^{\pm}\to\pi^{\pm}\pi^+\pi^-$ decay amplitude with $\pi^+\pi^-$ charge exchange to $\pi^0\pi^0$ is added as M_1 to the standard matrix element $M_0 \propto 1 + \frac{g_0}{2}u + \frac{h'}{2}u^2$ to give the simple re-scattering model parameterized as:

$$M \propto 1 + \frac{g_0}{2}u + \frac{h'}{2}u^2 + M_1(a_0, a_2, u)$$

Assuming isospin symmetry the additional term reads $M_1 = -2/3\,(a_0 - a_2) m_{\pi^+} M_+ \sqrt{(1 - M^2_{00}/2m_{\pi^+})}$

It contains the $\pi\pi$ scattering lengths (a_0, a_2) and M_+, the equivalent of M_0 for the standard $K^{\pm}\to\pi^{\pm}\pi^+\pi^-$ decay.

The interference between M_1 and M_0 is destructive below $M_{00} = 2m_{\pi^+}$ and constructive above when M_1 becomes imaginary. The specific effect of the cusp is clearly visible in the red circle of figure 6. Under the threshold there is a depletion which amounts to about 13% with respect to the "unperturbed" decay.

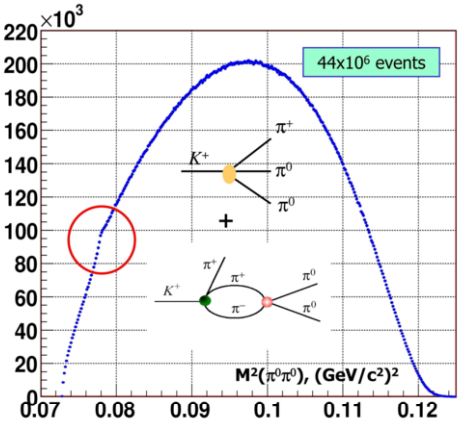

Fig 6: The cusp structure of the $\pi^0\pi^0$ invariant in $K^{\pm}\to\pi^{\pm}\pi^0\pi^0$ decay resulting from interference with the $K^{\pm}\to\pi^{\pm}\pi^+\pi^-$ decay with re-scattering. The distribution is from the data set taken in 2004.

3.3. Cusp analyzed.

The quantitative analysis of the cusp data is made in terms of the same quantities (a_0, a_2) in use for K_{e4}.

Cabibbo and Isidori (CI) have brought some refinement to the original model that now includes all re-scattering processes at the one-loop and two-loop level [15]. An independent approach at the two loop level and including electromagnetic effects is available from Colangelo, Gasser, Kubis and Rusetski (CGKR) [16]. It uses effective field theory and is based on non-relativistic Lagrangian.

The corrections due to isospin symmetry breaking are taken into account and applied for all $\pi\pi\to\pi\pi$ scattering amplitudes with different combination of electric charges of the pions. From the combined samples 2003/2004 a total of about 60×10^6 events is now used for the measurement of (a_0, a_2) by fitting the one dimensional u distribution with the matrix element M and by taking into account the acceptance and resolution functions calculated by Monte Carlo simulation.

The rescattering model described with M does not include an important type of radiative corrections, which are important near $M_{00} = 2m_{\pi^+}$, namely those that contribute to the formation of *pionium*.

This *pionium* signal is seen in $K^{\pm}\to\pi^{\pm}\pi^0\pi^0$ decays as shown in figure 7 by the deviation between data and Monte Carlo clearly visible in the vicinity of the threshold. Seven bins around the cusp point are excluded from the fit to reduce the potential dependence from electromagnetic effects in the *pionium* region. Nonetheless the excess of events above continuum seen around $M_{\pi^0\pi^0} = 2m_{\pi^+}$ is explained as *pionium* signature to a large extent. The observed yield is about two times higher than the theoretical prediction of *pionium* production [17] and some additional contribution is expected from electromagnetic effects [18] at a level of about half of the "unexplained" excess.

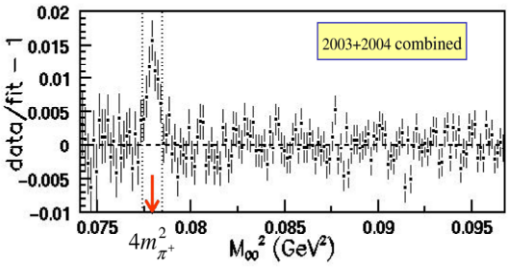

Fig 7: The fit of $K^{\pm}\to\pi^{\pm}\pi^0\pi^0$ with $\pi\pi$ re-scattering from the $K^{\pm}\to\pi^{\pm}\pi^+\pi^-$ decay. The excess of events around the red arrow is mostly *pionium* production and the 7 bins in this region are not used in the fit.

The cusp analysis is made with both the CI model and the CGKR model. This χPT constraint fit is done with 1 parameter, (a_0-a_2), with the results:

$$a_0 - a_2 = 0.268 \pm 0.003(stat) \pm 0.002(syst) \pm 0.001(ext)$$
$$a_0 - a_2 = 0.266 \pm 0.003(stat) \pm 0.002(syst) \pm 0.001(ext)$$

for CI and CGKR respectively.

Similarly for the 2 parameter fit with (a_0-a_2) and a2 the result with CI model is:

$$a_0 - a_2 = 0.266 \pm 0.005(stat) \pm 0.002(syst) \pm 0.001(ext)$$
$$a_2 = -0.039 \pm 0.009(stat) \pm 0.006(syst) \pm 0.002(ext)$$

And with CGKR model:

$$a_0 - a_2 = 0.273 \pm 0.005(stat) \pm 0.002(syst) \pm 0.001(ext)$$
$$a_2 = -0.065 \pm 0.015(stat) \pm 0.010(syst) \pm 0.002(ext)$$

The external error quoted for both models comes mostly from the error in the ratio of weak amplitudes of $K^{\pm}\to\pi^{\pm}\pi^+\pi^-$ and $K^{\pm}\to\pi^{\pm}\pi^0\pi^0$ decay.

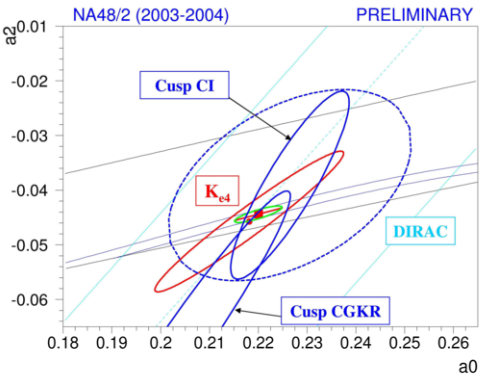

Fig 8: The scattering lengths a_0 and a_2 from cusp structure in $K^{\pm}\to\pi^{\pm}\pi^0\pi^0$ decays fitted with CI and CCKR models. The blue dotted ellipse has 5% theoretical error in CI as due to some higher order terms that are still neglected.

The cusp effect in $K^{\pm}\to\pi^{\pm}\pi^0\pi^0$ decays provides another precise measurement of the scattering lengths, totally independent from the K_{e4}. The good agreement between the two results is shown in figure 8 together with the theoretical calculation is which is now strongly established.
Another determination of (a_0, a_2) consistent with the NA48/2 measurements is provided by the measurement of the lifetime of $\pi\pi$ atoms detected by the DIRAC collaboration [19] under different conditions conducted by the DIRAC Collaboration. All the determinations of a_0 are summarized in figure 9.

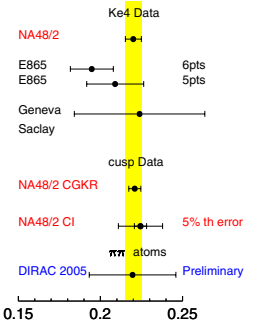

Fig 9: The $\pi\pi$ scattering length a_0 measured by different experiments.

This excellent agreement between theory and experiment on a_0 and a_2 is strong support [20] [21] to the GMOR theory in which the quark condensate is the dominant source giving mass to the pions.

4. Conclusion.

The NA48/2 experiment has made two independent measurements of $\pi\pi$ scattering lengths that are in very good agreement. These measurements of a_0 and a_2 have benefited a great deal from theoretical calculations. These predictions based on χPT are done at one and two-loop level to take into account re-scattering effects. The scattering lengths have been extracted from K_{e4} and $K^{\pm}\to\pi^{\pm}\pi^0\pi^0$ cusp data, give a consistent experimental picture and are in striking agreement with predictions from χPT:

$$a_0 = 0.220 \pm 0.005$$

The reach of such precision in hadronic physics is quite unusual. The experimental results have now reached the same accuracy as χPT and they confirm the hypothesis that the quark condensate is the leading order parameter of spontaneous symmetry breaking in QCD [19].

Acknowledgements

It was a great pleasure to participate to the 8th BEACH Conference held at the University of Columbia SC. Many thanks are due to the organizers for the wonderful organization of this stimulating meeting and the invaluable help and kindness that they provided to their guests.

References

1. V. Fanti *et al*. NIM **A574**, 433-471, (2007)
2. J. Batley *et al*, Eur.Phys. J. C52, 875--891 (2007)
3. L. Rosselet *et al*, Phys.Rev. **D15** (1977) 574.
4. S. Pislak *et al*, Phys.Rev. Lett. **87** (2001) 221801, Phys. Rev. **D67** (2003) 072004.
5. N. Cabibbo and A. Maksymovicz, Phys.Rev. **137** (1965) B438, Phys. Rev. **168** (1968) 1926.
6. T.D. Lee and C.S. Wu, Ann.Rev.Nucl.Sci **16** (1966) 471.
7. A. Pais and S. Treiman, Phys.Rev. **168** (1968) 1858.
8. J. Gasser, arXiv 0710.3048
9. S. Roy, Phys.Lett. **B36** (1971) 353.
10. B. Ananthanarayan, G. Colangelo, J. Gasser and H. Leutwyler, Phys. Rep. **353 (**2001**)** 207.
11. S. Descotes-Genon, N. Fuchs, L. Girlanda and J. Stern, Eur. Phys. J. **C 24 (**2002**)** 469
12. G. Colangelo *et al*, Nucl.Phys. **B603** (2001) 125.
13. J.R. Batley *et al*, Phys.Lett. **B633**, 173 (2006)
14. N. Cabibbo, Phys.Rev.Lett. **93** 121801 (2004)
15. N. Cabibbo and G. Isidori, JHEP **503** 21 (2005)
16. G. Colangelo, J. Gasser, B. Kubis and A. Rusetkky, Phys.Lett. **B638** (2006)
17. Z. Silagadze, JETP Lett. 60 689 (1994).
18. S. Gevorkyan *et al*, Phys.Lett. **B649** 159 (2007).
19. B. Adeva *et al*, Phys. Lett. **B619. (**2005**)**
20. G. Colangelo, J. Gasser and H. Leutwyler, Phys.Rev.Lett. **86** 22 (2001).
21. G. Colangelo, arXiv:hep-ph/05001107 (2005)